Aerosol Science and Technology

ISSN: 0278-6826 (Print) 1521-7388 (Online) Journal homepage: https://www.tandfonline.com/loi/uast20

Intercomparison Study of the Size-Dependent Counting Efficiency of 26 Condensation Particle Counters

A. Wiedensohlet , D. Orsini , D. S. Covert , D. Coffmann , W. Cantrell , M. Havlicek , F. J. Brechtel , L. M. Russell , R. J. Weber , J. Gras , J. G. Hudson & M. Litchy

To cite this article: A. Wiedensohlet , D. Orsini , D. S. Covert , D. Coffmann , W. Cantrell , M. Havlicek , F. J. Brechtel , L. M. Russell , R. J. Weber , J. Gras , J. G. Hudson & M. Litchy (1997) Intercomparison Study of the Size-Dependent Counting Efficiency of 26 Condensation Particle Counters, Aerosol Science and Technology, 27:2, 224-242, DOI: 10.1080/02786829708965469

To link to this article: https://doi.org/10.1080/02786829708965469

Published online: 13 Jun 2007.

Intercomparison Study of the Size-Dependent Counting Efficiency of 26 Condensation Particle Counters

A. Wiedensohlet, D. Orsini, D. S. Covert, D. Coffmann, W. Cantrell, M. Havlicek, F. J. Brechtel, L. M. Russell, R. J. Weber,† J. Gras, J. G. Hudson, and M. Litchy*

INSTITUTE FOR TROPOSPHERIC RESEARCH, PERMOSERSTRASSE 15, D-04303 LEIPZIG, GERMANY (A. W., D. O.); UNIVERSITY OF WASHINGTON, DEPARTMENT OF ATMOSPHERIC SCIENCE, 4909 25TH AVE, NE, SEATTLE, WA 98195-4235, USA (D. S. C., D. C.); GEOPHYSICAL INSTITUTE, UNIVERSITY OF ALASKA, FAIRBANKS, AK 99775-7320, USA (W. C.); TSI INCORPORATED, 500 CARDIGAN ROAD, P.O. BOX 64394, ST. PAUL, MN 55164, USA(M. H.); COLORADO STATE UNIVERSITY, DEPARTMENT OF ATMOSPHERIC SCIENCE, FT. COLLINS, CO 80523, USA (F. J. B.); CALIFORNIA INSTITUTE OF TECHNOLOGY, DEPARTMENT OF CHEMICAL ENGINEERING, PASADENA, CA 91125, USA (L. M. R.); UNIVERSITY OF MINNESOTA, DEPARTMENT OF MECHANICAL ENGINEERING, MINNEAPOLIS, MN 55455-0111, USA (R. J. W.); CSIRO, DIVISION OF ATMOSPHERIC RESEARCH, PMB 1, MORDIALLOC, VIC 3195, AUSTRALIA (J. G.); DESERT RESEARCH INSTITUTE, 5625 FOX AVE., RENO, NV 89506-0220, USA (J. G. H.); UNIVERSITY OF HAWAII, DEPARTMENT OF OCEANOGRAPHY, HONOLULU, HI 96822, USA (M. L.)

ABSTRACT. Particle detection efficiency curves for 26 condensation particle counters were determined during a calibration workshop in preparation for the Aerosol Characterization Experiment 1 (ACE1). Three different types of commercially available particle counters, the ultrafine condensation particle counter (TSI-3025) and the condensation particle counters (TSI-3010 and TSI-3760 or TSI-7610) were investigated at default temperature and flow settings as well as for other flow rates and temperature differences between the saturator and the condenser. Furthermore, the pulse-height-analysis ultrafine condensation particle counter and a TSI-3010 modified to achieve a higher temperature difference were calibrated. In this study, the large number of particle counters investigated provided the opportunity to obtain a more statistically significant picture of the performance of different particle counters for different operating conditions. AEROSOL SCIENCE AND TECHNOLOGY 27:224–242 (1997)

INTRODUCTION

Condensation particle counters (CPC) are widely used for measuring the number concentration of submicrometer aerosol particles. Applications include measurements of total aerosol number concentrations (limited by the 50% detection efficiency diameter of the particle counter), or the number concentration measurements after sizing devices such as differential mobility analysers (DMA) or diffusion batteries. Particle counters used in state-of-the-art

* Corresponding author.
† New address: Brookhaven National Laboratory, Atmospheric Chemistry Division, Upton, NY 11973.

0278-6826/97/$17.00
PII S0278-6826(97)00008-1

Aerosol Science and Technology 27:224–242 (1997)

Published by Elsevier Science Inc.

techniques are based on the continuous flow, single-particle-counting CPC principle as described by Agarwal and Sem (1980).

In this study, the particle detection efficiency curves and 50% particle detection efficiency diameters were measured for three commercially available continuous flow CPCs [CPC TSI-3760, CPC TSI-3010, and the ultrafine condensation particle counter (UCPC) TSI-3025], the pulse-height-analysis UCPC (PHA-UCPC; originally, the prototype of the TSI-3025 UCPC), and a modified CPC TSI-3010. Since the CPCs were to be used during the Aerosol Characterization Experiment 1 (ACE1) field campaign (Nov.–Dec. 1995) in Tasmania, Australia, the calibrations were performed under the operating conditions (i.e., flow rate and temperature difference between saturator and condenser) planned for ACE1.

The particle counting efficiency curve for the UCPC TSI-3025 has been presented in a recent publication. In Kesten et al. (1991), the counting efficiency curve was measured with silver and sodium chloride as particle materials. They found a relatively steep detection efficiency curve with a counting efficiency larger than 95% for particle diameters $D_p > 6$ nm. The 50% detection efficiency diameters observed for silver and sodium chloride were 2.90 and 3.14 nm, respectively. The aerosol was produced in a tube furnace generator (Scheibel and Porstendörfer, 1983) and size-segregated by TSI-3071 differential mobility analyzer (DMA). A TSI-3068 aerosol electrometer was used as a comparison standard.

The counting efficiency curve and the 50% detection efficiency of the PHA-UCPC have been investigated previously by Stolzenburg and McMurry (1991) employing sodium chloride particles, and again by Weber (1995) with sodium chloride tungsten oxide, sulphuric acid, and ammonium sulphate as particle materials. For the PHA-UCPC, counting efficiencies for particles larger than 3 nm were compared at $p = 250$, 500, 670, and 1000 mbar. It was found that the counting efficiency dropped only slightly with decreasing pressure for particles between 3 and 6 nm. The counting efficiency was insensitive to pressure changes for particles >6 nm (Saros et al., 1996).

Recent studies by Fissan et al. (1996) and Birmili et al. (1997) have shown that the DMA transmission function for ultrafine particles <10 nm became relatively broad. The broad DMA mobility bins lead to larger uncertainties in the counting efficiency in the particle size range where the counting efficiency curve is steepest.

The nominal 50% particle detection efficiency diameter of the TSI-3010 CPC is approximately 10 nm for the standard flow rate of 1.0 l/min and the default temperature difference, ΔT, between saturator and condenser of 17°C. In Mertes et al. (1995), the particle detection efficiency curve for three ΔTs, 17, 21, and 25°C was measured at the standard flow rate. The 50% particle detection efficiency diameters determined by Mertes et al. (1995) were 10.5, 7.6, and 5.7 nm, respectively. In other words, with decreasing temperature difference ΔT, the 50% detection efficiency diameter was shifted to smaller particle sizes. Furthermore, the slope of particle detection efficiency curve became steeper with increasing ΔT. Here, two UCPC-TSI 3025s with a nominal 50% particle detection efficiency diameter of 3 nm were used as comparison detectors. They assumed that the TSI-3025 UCPC performed the same as the UCPC which Kesten et al. (1991) compared to an electrometer. Thus, their standard was an electrometer with the UCPC as the transfer standard and the assumption that two UCPCs have identical efficiencies down to 4 nm in particle diameter. A Hauke-type DMA was used to select a quasi-monodisperse ultrafine aerosol from a tube furnace generator. The DMA was operated with a 3/20 aerosol-to-sheath air flow ratio.

The TSI-3010 is designed to maintain a constant temperature difference ΔT, while the absolute temperatures of the saturator and condenser may vary. The maximum

ΔT, which may currently be set for the TSI-3010, is 25°C. A larger ΔT was reached for the modified TSI-3010 by adding active heating of the saturator and thermal decoupling of the saturator (bottom part of the CPC) from the condenser block. The counting efficiency of the modified TSI-3010 CPC was investigated down to 5 nm in diameter by Russell et al. (1996) with silver and sodium chloride particles.

The TSI-3760 CPC (equivalently, the TSI-7610 CPC) has a nominal 50% particle detection efficiency diameter of 15 nm for a standard flow rate of 1.416 l/min (0.05 ft^3/min). Zhang and Liu (1991) published particle detection efficiency curves for this particle counter for reduced pressures and flow rates using an aerosol electrometer as a comparison detector. They confirmed the 50% particle detection efficiency diameter for standard pressure (1013 mbar) and standard flow rate conditions. Furthermore, they found that the counting efficiency curve was shifted to larger sizes with decreasing pressure and flow rates. In a study by Hermann and Wiedensohler (1996), the counting efficiency was measured down to 200 mbar. They found, in contrast to Zhang and Lui (1991), a shift of the particle detection efficiency curve toward smaller sizes with decreasing pressure. For 200 mbar, the 50% detection efficiency was found to be 12 nm.

The CPC calibration workshop held in Seattle, August 1995, in preparation for the ACE1 field campaign 1995, provided the unique opportunity to compare the performance of several particle counters of the same type. A total of 26 CPCs from 10 different institutes (6 TSI-3025, 11 TSI-3010 including the modified version, 8 TSI-3760 or TSI-7610, and the PHA-UCPC) were calibrated under the operating conditions planned for the ACE1 field measurements. The goals of the workshop were twofold. First, to test and correct for possible problems within each counter. Second, to measure and calibrate the counting efficiencies of each CPC, thereby allowing for data intercomparisons among the different planned measuring platforms of the ACE1 experiment.

DESCRIPTION OF THE CONDENSATION PARTICLE COUNTER CALIBRATION

The calibration of the particle counters was performed with the experimental setup shown in Fig. 1. The monodisperse ultrafine aerosol generator consisted of a tube furnace for generating a polydisperse ultrafine aerosol ($\sigma_g \sim 1.4$), a bipolar charger (neutraliser TSI-3077), and an ultrafine DMA (Hauke type VIE-06) for selecting particles of known size from the furnace-generated

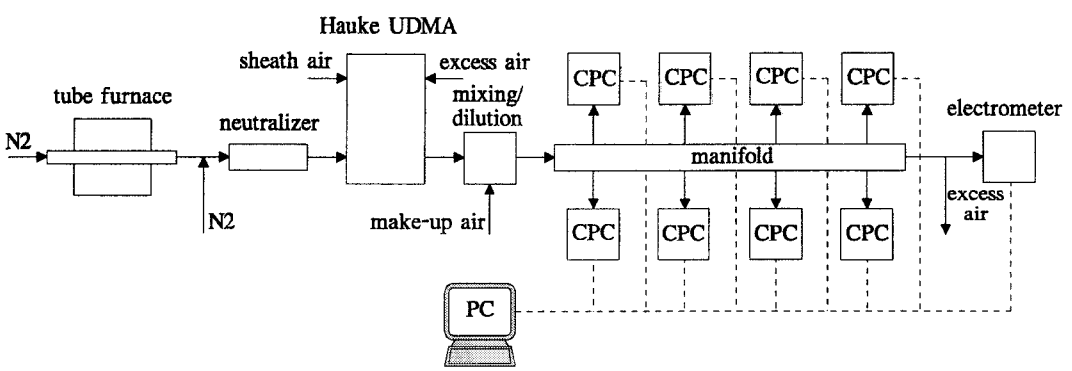

FIGURE 1. Experimental setup used during the CPC intercalibration workshop.

aerosol. This approach for generating monodisperse ultrafine silver aerosols was originally described by Scheibel and Porstendörfer (1983). Silver particles were used to avoid effects of hygroscopic growth on the counting efficiency which could be induced by variations of the relative humidity of the sample flow. The monodisperse aerosol was mixed afterward with particle-free air and distributed to the particle counters (maximum eight at one time) from a sampling manifold. The tubing lengths were kept constant between the manifold and each CPC to ensure that the diffusional losses of ultrafine particles were the same for each particle counter. Special attention was also given to precise setting of the aerosol flow rates. This was especially the case with the TSI-3025 UCPC, where instrument limitations cause an uncertainty of at least ±10% in the aerosol sample flow.

Six TSI-3025 UCPCs were calibrated under standard conditions, i.e., $\Delta T = 27°C$ and "high flow" mode (1.5 l/min total flow rate, 0.03 l/min aerosol sample flow rate) in the size range 2.5–10 nm. Additionally, the PHA-UCPC was calibrated ("high flow" mode, $\Delta T = 31°C$, 0.03 l/min aerosol sample flow rate) and the modified TSI-3010 ($\Delta T = 36°C$ and 1 l/min aerosol flow rate) for the ultrafine particle size range (Table 1).

We decided to calibrate to two TSI-3025 UCPCs against an electrometer and to employ them as reference detectors for the other CPCs. There were several reasons for this decision: (a) to calibrate the CPCs for number concentrations around 1000 cm^{-3}, (b) to avoid coincidence, (c) to avoid low electrometer readings, and (d) to calibrate several CPCs at once.

The particle detection efficiencies of two TSI-3025 UCPCs (12 and 13) were used as relative reference efficiencies. This was accomplished with a comparison against a set of six TSI-3010 CPCs. The reason for this intercomparison was the existence of uncertainties of ±10% in the aerosol flow of the TSI-3025 UCPCs. Furthermore, the TSI-3010 CPCs were originally calibrated against the manufacturer's standard electrometer. This means that the reference UCPC and, thus, all CPCs would be calibrated against the manufacturer's standard.

First, the flow rates of the TSI-3010 CPCs were adjusted to be exactly 1.0 l/min. Due to the good counting statistic of a TSI-3010 CPC (resulting from the relatively high aerosol flow rate) compared to a TSI-3025 UCPC (0.03 l/min), it can be assumed that the counting efficiencies of the TSI-3010 CPCs were 100% for 40 nm particles. All TSI-3010 CPC number concentrations agreed within ±2%. The small deviations provided confidence that the precision of the TSI-3010 number concentration was high and, furthermore, that the aerosol was homogeneously mixed in the manifold. Finally, the flows of the 12 and 13 UCPCs and the other four TSI-3025 UCPCs were adjusted until agreement with all other TSI-3010 CPC's was found.

TABLE 1. Ultrafine Condensation Particle Counters Calibrated during the Intercomparison Workshop

CPC Number	CPC Type	Institute	Serial Number	Aerosol Flow rate (l/min)	Temperature Difference ΔT (°C)
9	TSI-3025	Colorado State Univ.	1091	0.03	27
10	TSI-3025	Pacific Marine Environmental Laboratory	1099	0.03	27
11	TSI-3025	Univ. of Hawaii	1011	0.03	27
12	TSI-3025	Univ. of Washington	1110	0.03	27
13	TSI-3025	Institute for Tropospheric Research	1109	0.03	27
14	TSI-3025	Univ. of Washington	1041	0.03	27
23	PHA-UCPC	Univ. of Minnesota	—	0.03	31
20	Modified TSI-3010	California Institute of Technology	2030	1.0	36

The absolute detection efficiency was measured using a TSI-EAA (electrostatic aerosol analyser) electrometer as the comparison detector with a lower detection limit of 10^{-15} A. The electrometer showed a positive gain error of 9.2%. This deviation (mean value derived from comparison of the electrometer number concentration with both reference counters) was found to be relatively constant with particle size (20, 30, and 40 nm). The counting efficiencies of both reference UCPCs were corrected for this gain error in the size range 2.5–10 nm. The measured particle detection efficiences of the UCPCs 12 and 13 compared with exponential two-parameter fits Eq. 1 are plotted in Fig. 2a. The two-parameter equation

$$\eta = 1 - \exp\left((D_0 - D_p)/D_2\right), \qquad D_p \geq D_0,$$
$$\eta = 0, \qquad D_p \leq D_0. \tag{1}$$

was developed by Stolzenburg and McMurry (1991) to describe the condensation activation efficiency neglecting the sampling efficiency. For this study, however, the two-parameter fit was sufficient to fit the measurements.

In the next step, the four other TSI-3025 UCPCs, the PHA-UCPC, and the modified TSI-3010 CPC were calibrated against the UCPCs 12 and 13 in the 2.5–10 nm particle size range. The exponential fit of the UCPC 12 counting efficiency was used to calculate the particle detection efficiency of the other particle counters from the comparison measurements. For the data interpretation, the measured particle detection efficiencies were normalised to unity for 10 nm particles. The measured (crosses) and normalised counting efficiencies (solid squares) of the TSI-3025 UCPCs 9, 10, 11, and 14 compared with exponential fits (solid lines) are plotted in Fig. 2b–e, respectively. As one can recognise, the aerosol flow rate probably drifted from the value set in the UCPC calibration leading to counting efficiencies larger or smaller than unity for 10 nm. The TSI-3025 UCPCs 9, 10, 11, and 14 show fairly sharp efficiency cutoffs consistent with the results of Kesten et al. (1991). These counting efficiency curves are also comparable with the measured counting efficiency of the PHA-UCPC as shown later.

The remaining two TSI-3015 UCPCs 12 and 13 from this study showed degraded performance with much broader efficiency cutoff characteristics. The sharpness of the efficiency cutoff of a properly functioning UCPC (beside particle material effects) is achieved by containing the aerosol flow close to the centre line of the condenser tube where the supersaturation is highest. It might be that the cause for the broadening of the counting efficiency curve is a disruption of the axially symmetric laminar flow in the condenser tube. This could result from dirt on the surface of the aerosol injection capillary near the trailing knife edge. Here, the aerosol and the sheath flow must smoothly merge. A short way upstream, the sheath air flow must pass through a narrow annular gap through which condensed butanol must flow down the wall in the opposite direction. If a drop of butanol bridges this gap, it could also upset the axial symmetry of the sheath air flow. Furthermore, misalignment of the aerosol sample injection assembly could cause similar problems.

Figure 2a–e and the parameterized fits given in Table 2 indicate that TSI-3025 UCPC 12 and 13 are outliners. It seems that such flow disturbance occurred unfortunately in the reference UCPCs. Therefore, the average counting efficiency curve was calculated from the normalised counting efficiency of the four TSI-3025 UCPCs (9, 10, 11, and 14). The average measurement (solid squares) is compared with a two-parameter fit (solid line) through the measure data (Fig. 3). Additionally, the width of the DMA size bins (horizontal bars) derived from the DMA calibration study by Birmili et al. (1997) and the maximum and minimum measured counting efficiencies (vertical bars) are given in Fig. 3. The horizontal bars demonstrate the uncertainty in the counting efficiency due to the width of the DMA mobility bin in the

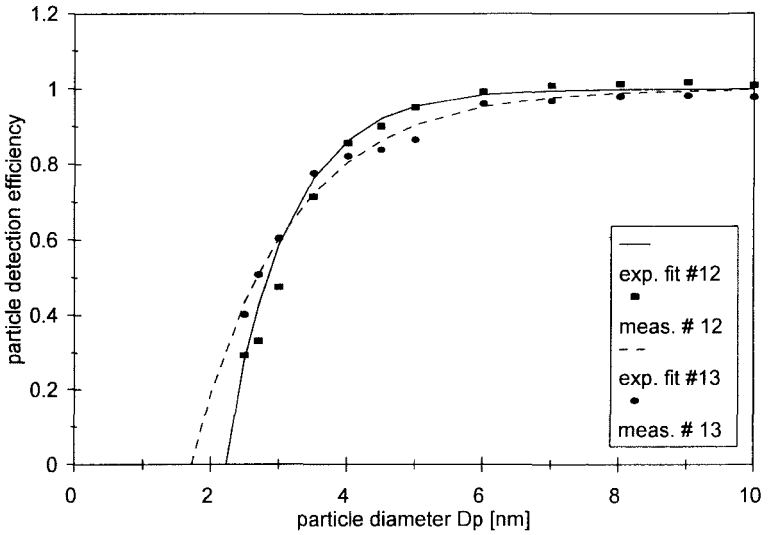

(a)

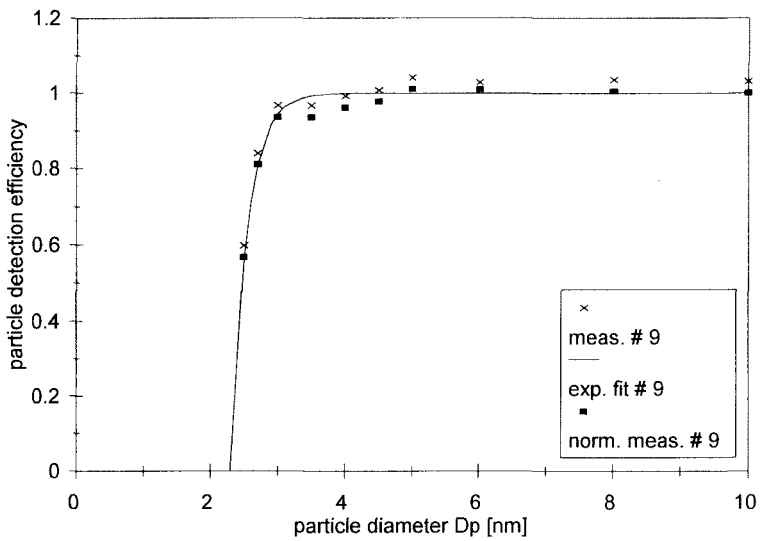

(b)

FIGURE 2. (a) Counting efficiency curve of two TSI-3025 UCPCs determined in comparison with an aerosol electrometer. The open squares and the solid circles represent the normalised particle detection efficiency of UCPCs 12 and 13, respectively. The solid and the dashed lines represent two-parameter exponential fits of the measurements. (b)–(e) Measured (crosses) and normalised (100% for 10 nm; solid squares) counting efficiencies of the TSI-3025 UCPCs (9, 10, 11, and 14) compared with two-parameter exponential fits (solid lines).

size range 2.5–3.5 nm where the counting efficiency curve is relatively steep.

The fitted detection efficiency curves of the TSI-3025 UCPC for silver as a particle material determined in this study (solid line) and in the investigation by Kesten et al. (1991) (dashed line) are shown in Fig. 4. The counting efficiency curves determined by using silver as a particle material are very similar. The average 50% counting

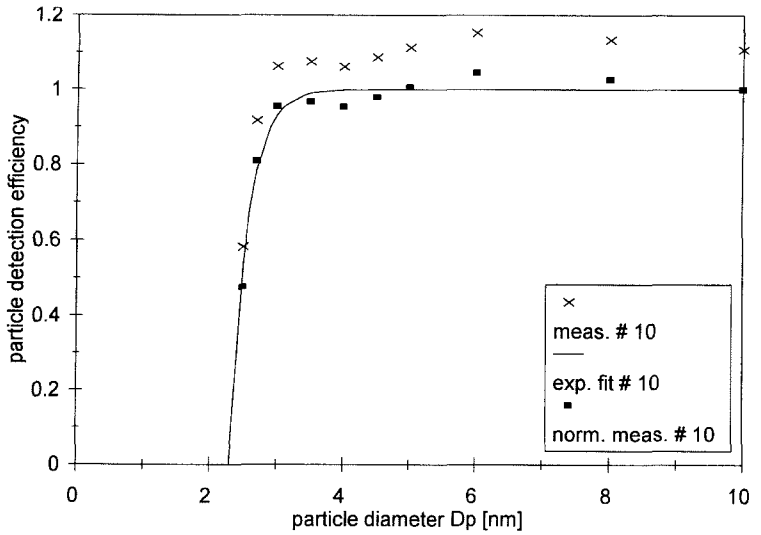

(c)

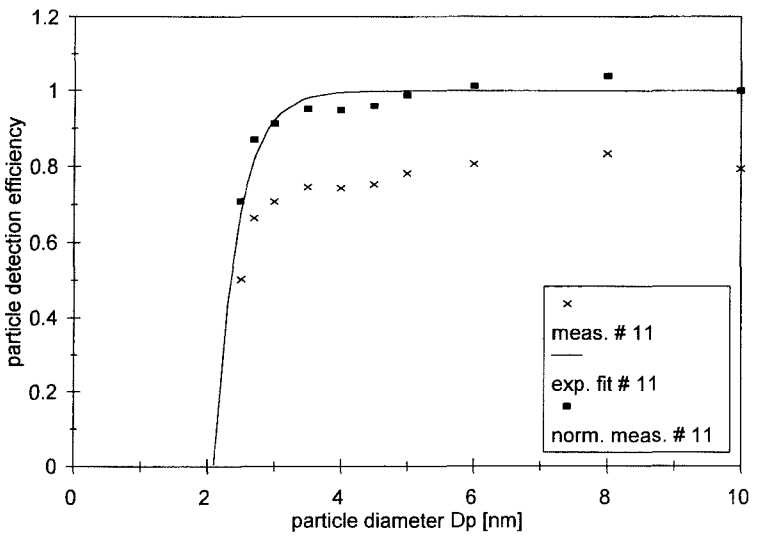

(d)

FIGURE 2. (*continued*)

efficiency diameter (2.42 nm) in this study, however, is slightly smaller than the 50% counting efficiency (2.90 nm) found by Kesten et al. This difference is in the uncertainty range of the DMA transfer functions. In their study, Kesten et al. (1991) used a TSI DMA model 3071 that probably had a broader width of the transfer function for particles <5 nm in diameter. As a comparison, the particle detection efficiency for sodium chloride (Kesten et al. 1991) as a particle material (dotted line) is plotted in Fig. 4 to illustrate the dependency of the counting efficiency of the TSI-

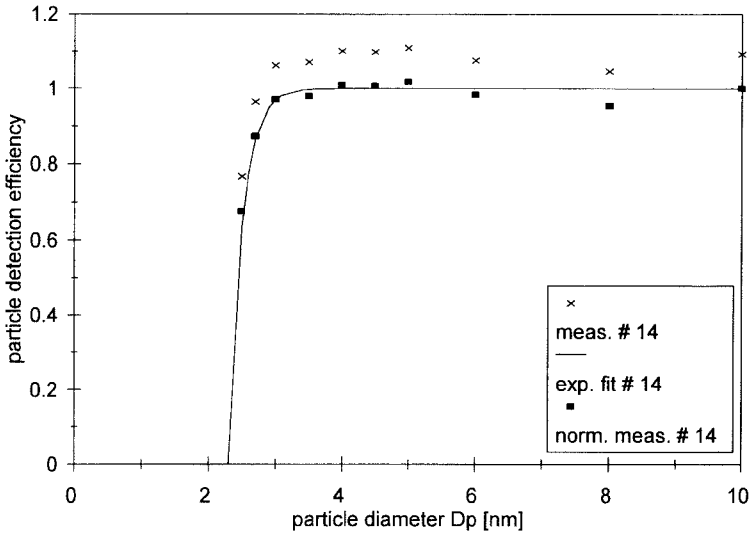

(e)

FIGURE 2. (*continued*)

3025 on the particle material in the size range <5 nm.

In Fig. 5, the measure and fitted particle detection efficiency curves for the different types of ultrafine particle counters investigated in this study are shown. The counting efficiency curve (solid circles and dashed line) of the PHA-UCPC is as steep as the average particle detection efficiency obtained from the TSI-3025 UCPCs (solid squares and solid line). The observed 50% counting efficiency is found to be 2.49 nm.

The ability of the modified TSI-3010 CPC (solid triangles and dotted line) to count much smaller particles than a standard TSI-3010 CPC is illustrated by the 50% counting efficiency diameter of only 3.75 nm. The coefficients for Eq. 1 for the fitted detection efficiency curves are summarised in Table 2.

TABLE 2. Coefficients of the Exponential Fit of Counting Efficiency Curves of the TSI-3025 UCPCs, the PHA-UCPC, and the Modified TSI-3010

CPC Number	CPC Type	$D_{p,0}$ (nm)	$D_{p,2}$ (nm)	$D_{p,50}$ (nm)
Average (9, 10, 11, 14)	TSI-3025	2.22	0.28	2.42
9	TSI-3025	2.30	0.24	2.47
10	TSI-3025	2.30	0.26	2.48
11	TSI-3025	2.10	0.35	2.34
12	TSI-3025	2.20	0.90	2.82
13	TSI-3025	1.70	1.40	2.67
14	TSI-3025	2.30	0.20	2.44
23	PHA-UCPC	2.35	0.20	2.49
20	Modified TSI-3010	2.00	2.50	3.75

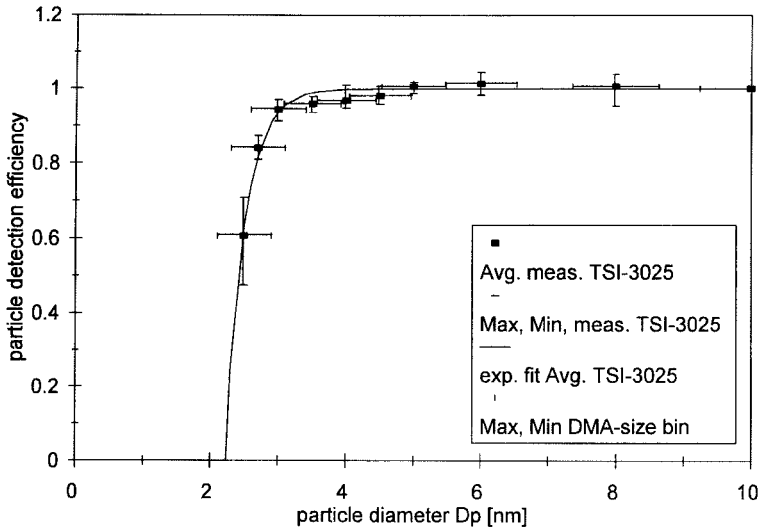

FIGURE 3. The average measured (solid squares) and fitted (solid line) counting efficiency curve obtained for the TSI-3025 UCPCs. The vertical bars represent the maximum and the minimum measured counting efficiencies and the horizontal bars represent the width of the DMA size bin.

Ten TSI-3010 particle counters were investigated in terms of their counting efficiencies for nominal operating conditions, e.g., temperature difference between saturator and condenser, $\Delta T = 17°C$, and 1 l/min aerosol sample flow rate, in the size range up to 25 nm (Table 3). Additionally, the counting efficiencies of 4 of the 10 TSI-3010 particle counters were determined at $\Delta T = 22°C$.

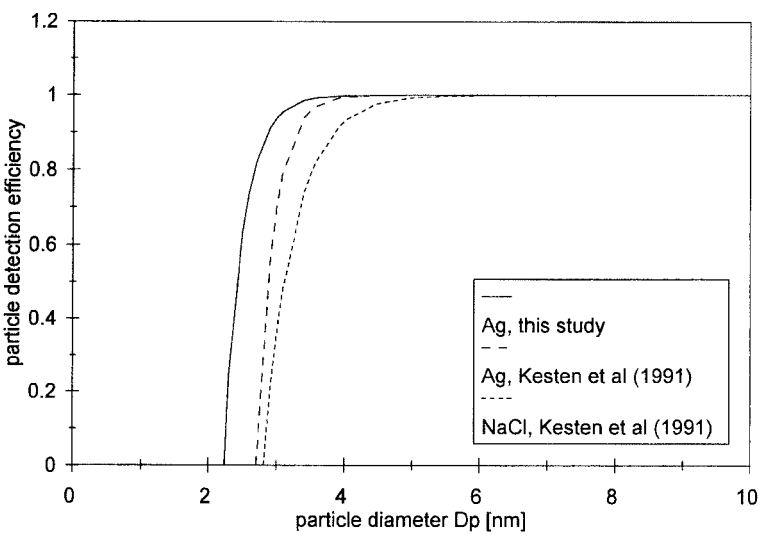

FIGURE 4. The average counting efficiency curve of the TSI-3025 UCPC obtained in this study (solid line) compared to previous results. The dashed and dotted lines represent Kesten's results for silver and sodium chloride, respectively.

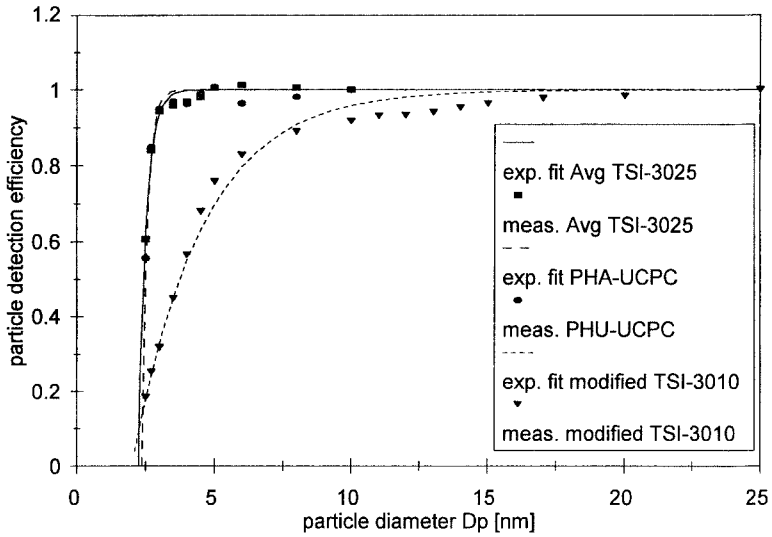

FIGURE 5. The average measured and fitted counting efficiencies of the TSI-3025 (solid squares and solid line) compared to the particle detection efficiencies of the PHA-UCPC (solid circles and dashed line) and the modified TSI-3010 (solid triangles and dotted line).

The measured particle detection efficiencies of the 10 TSI-3010 CPCs operated with $\Delta T = 17°C$ compared with a four-parameter exponential fits (Eq. 2) are plotted in Figure 6a (7, 8, 3), b (1, 4, 5), and c (2, 6, 17, 26). The variation of the counting efficiency curves is relatively small between the individual counters except one outlier (26). This CPC was employed in a previous study to count high concentrations of soot particles. The soot might be the reason for poorer 50% detection efficiency compared to the other TSI-3010 CPCs. The average measured counting efficiency (solid squares) of the TSI-3010 CPCs for $\Delta T = 17°C$ and a four-parameter fit (solid line) is plotted in Fig. 7. The horizontal bars describe the maximum and minimum measured counting efficiencies. The average counting efficiency for a ΔT of 17°C was derived using

TABLE 3. TSI-3010 CPCs Calibrated During the Intercomparison Workshop

CPC Number	CPC Type	Institute	Serial Number	Aerosol Flow Rate (l/min)	Temperature Difference ΔT (°C)		
1	TSI-3010	Univ. of Washington	2082	1.0	17	22	—
2	TSI-3010	Institute for Tropospheric Research	2040	1.0	17	—	—
3	TSI-3010	Institute for Tropospheric Research	2024	1.0	17	—	—
4	TSI-3010	Institute for Tropospheric Research	2006	1.0	17	—	—
5	TSI-3010	Colorado State Univ.	2023	1.0	17	22	—
6	TSI-3010	Univ. of Alaska, Fairbanks	2090	1.0	17	—	—
7	TSI-3010	Univ. of Washington	2086	1.0	17	22	—
8	TSI-3010	Univ. of Washington	2039	1.0	17	22	—
17	TSI-3010	Univ. of Hawaii	2010	1.0	17	—	—
26	TSI-3010	Desert Research Institut	2018	1.0	17	—	—
20	TSI-3010	California Institute of Technology	2030	1.0	—	—	36

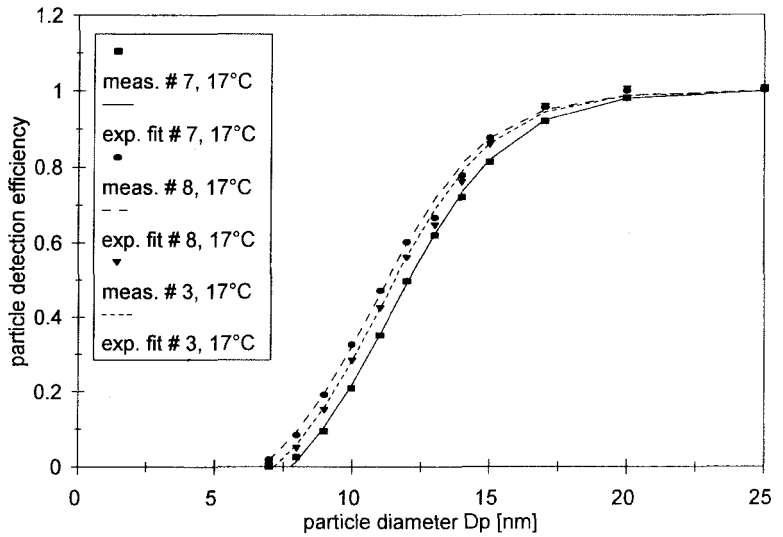

(a)

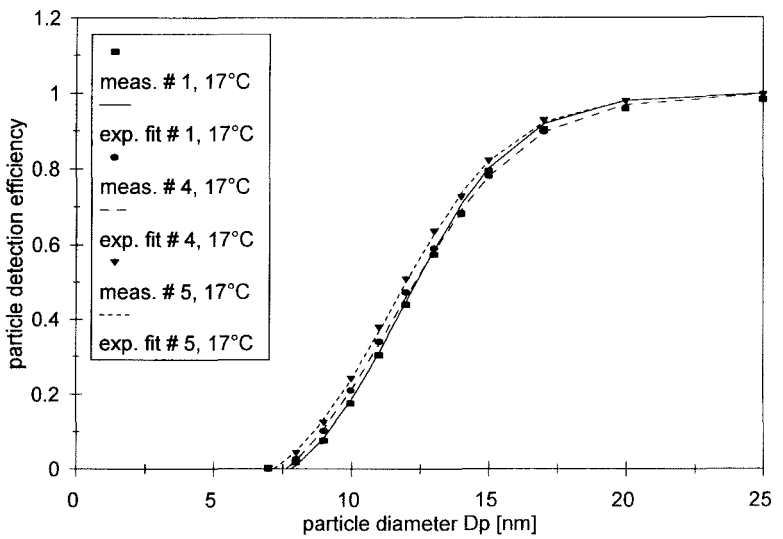

(b)

FIGURE 6. (a)–(c) The measured and fitted counting efficiencies of the TSI-3010 CPCs (7, 8, 3, 1, 4, 5, 2, 6, 17, and 26) for a temperature difference of 17° between saturator and condenser. The solid squares, circles, and triangles represent the measured counting efficiencies while four-parameter fits are represented by solid, dashed, dotted, and dashed-dotted lines.

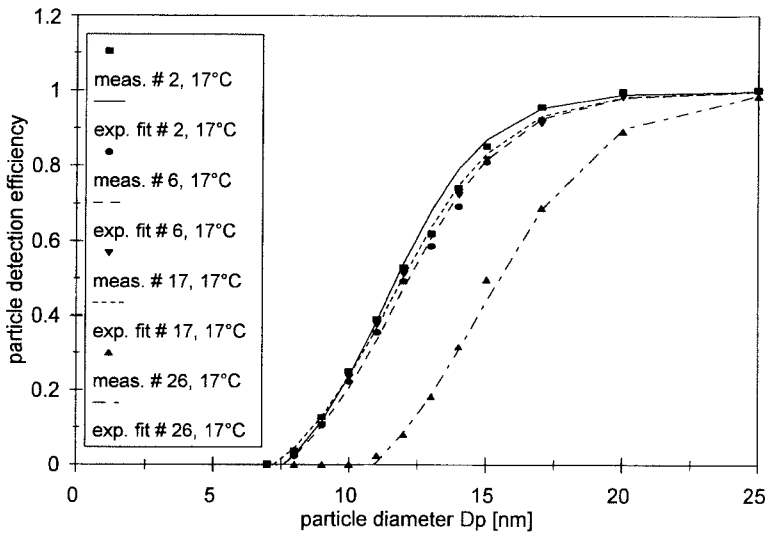

(c)

FIGURE 6. (*continued*)

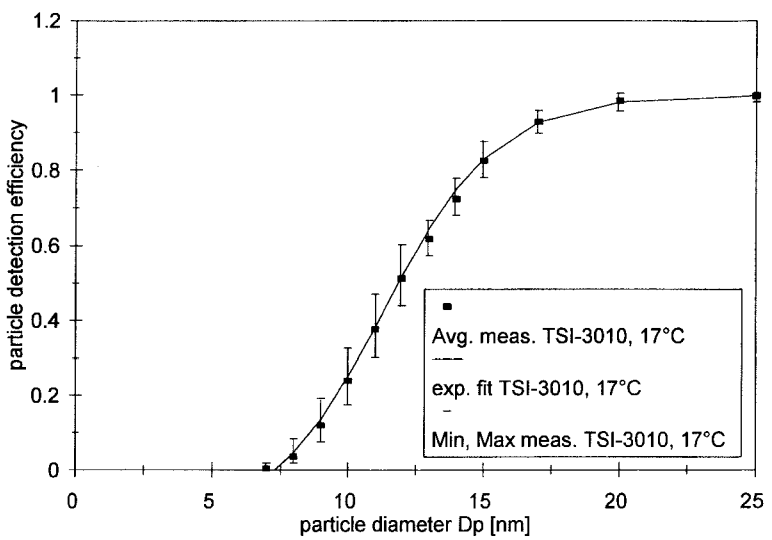

FIGURE 7. The average measured (solid squares) and fitted (solid line) particle detection efficiencies of the TSI-3010 CPC for a temperature difference of $\Delta T = 17°C$ between saturator and condenser. The horizontal bars represent the maximum and minimum measured counting efficiencies.

9 of the 10 calibrations. The outlier, CPC 26, was excluded. To describe the S-shape of the counting efficiency curve for these CPC's, the measured detection efficiency curve was fitted with the four-parameter exponential formula used in Mertes et al. (1995):

$$\eta = b - a \cdot \left(1 + \exp\left((D_p - D_1)/D_2\right)\right)^{-1}, \quad D_p \geq D_0,$$
$$\eta = 0, \quad D_p \leq D_0, \tag{2}$$

with $D_0 = D_2 \ln(a/b - 1) + D_1$.

The measured particle detection efficiencies of the four TSI-3010 CPCs (1, 5, 7, 8) operated with $\Delta T = 22°C$ compared with the four-parameter exponential fits (Eq. 2) are plotted in Figure 8. The average measured counting efficiency (solid squares) of the four TSI-3010 CPCs for $\Delta T = 22°C$ and a four-parameter fit (solid line) are plotted in Fig. 9. Again, the horizontal bars describe the maximum and minimum measured counting efficiencies. Here the variation of the counting efficiency curves for $\Delta T = 22°C$ is also relatively small between the individual counters.

The coefficients of the exponential fits and 50% detection efficiency diameters for the different counters and operating conditions are listed in Table 4. The average 50% detection efficiency diameters for $\Delta T = 22$ and 17°C were determined from the exponential fit to be 8.15 and 11.9 nm, respectively. These results are slightly different than the 50% detection efficiency diameters determined by Mertes et al. (1995) (10.5 nm) as well as the manufacturer's specification (10 nm) for $\Delta T = 17°C$. However, the trend of increased counting efficiency for smaller particles with increasing ΔT, as seen by Mertes et al. (1995), was confirmed. For comparison purposes, the counting efficiency curves for the different ΔTs (17, 22, and 36°C) obtained in this and

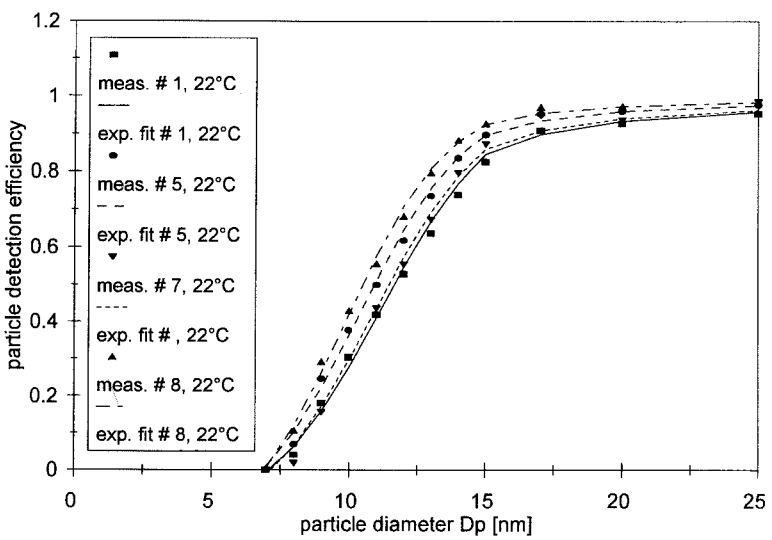

FIGURE 8. The measured and fitted counting efficiencies of the TSI-3010 CPCs (1, 5, 7, and 8) for a temperature difference of 22° between the saturator and condenser. The solid squares, circles, and triangles represent the measured counting efficiencies while four-parameter fits are represented by solid, dashed, dotted, and dashed-dotted lines.

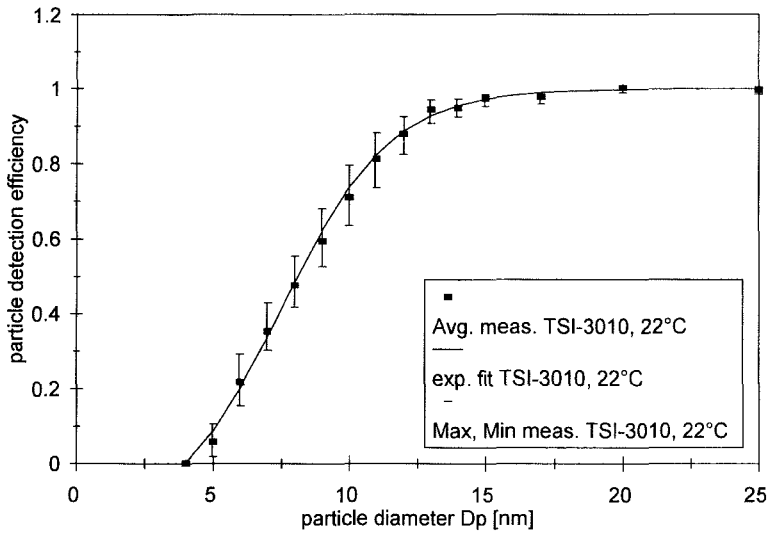

FIGURE 9. The average measured (solid squares) and fitted (solid line) particle detection efficiency of the TSI-3010 CPC for a temperature difference of $\Delta T = 22°C$ between saturator and condenser. The horizontal bars represent the maximum and minimum measured counting efficiencies.

in Mertes' investigation are plotted in Fig. 10. The performance of the modified TSI-3010 CPC is remarkable. As mentioned previously, the 50% detection efficiency diameter was found to be 3.75 nm. No homogeneous nucleation of butanol vapour that one could expect for a ΔT of 36°C was observed.

Eight TSI-3760/7610 CPCs were calibrated for different aerosol flow rates: three

TABLE 4. Coefficients of the Exponential Fit of Counting Efficiency Curves of the TSI-3010 CPCs for Different ΔT between Saturator and Condenser

CPC Number	CPC Type	ΔT (°C)	b	a	D_1 (nm)	D_2 (nm)	$D_{p,50}$ (nm)
Average (all except 26)	TSI-3010	17	1	1.15	11.3	2.1	11.90
1	TSI-3010	17	1	1.13	11.9	2.0	12.33
2	TSI-3010	17	1	1.13	11.3	1.8	11.72
3	TSI-3010	17	1	1.15	11.0	2.0	11.52
4	TSI-3010	17	1	1.18	11.6	2.3	12.18
5	TSI-3010	17	1	1.13	11.5	2.1	11.82
6	TSI-3010	17	1	1.13	11.7	2.0	12.06
7	TSI-3010	17	1	1.18	11.4	2.1	11.92
8	TSI-3010	17	1	1.13	10.8	2.0	11.32
17	TSI-3010	17	1	1.12	11.5	2.0	11.96
26	TSI-3010	17	1	1.17	14.8	2.2	15.23
Average	TSI-3010	22	1	1.17	7.5	2.0	8.15
1	TSI-3010	22	1	1.15	8.1	2.1	8.78
5	TSI-3010	22	1	1.18	7.3	2.0	7.97
7	TSI-3010	22	1	1.18	7.8	2.1	8.45
8	TSI-3010	22	1	1.22	6.8	1.9	7.49

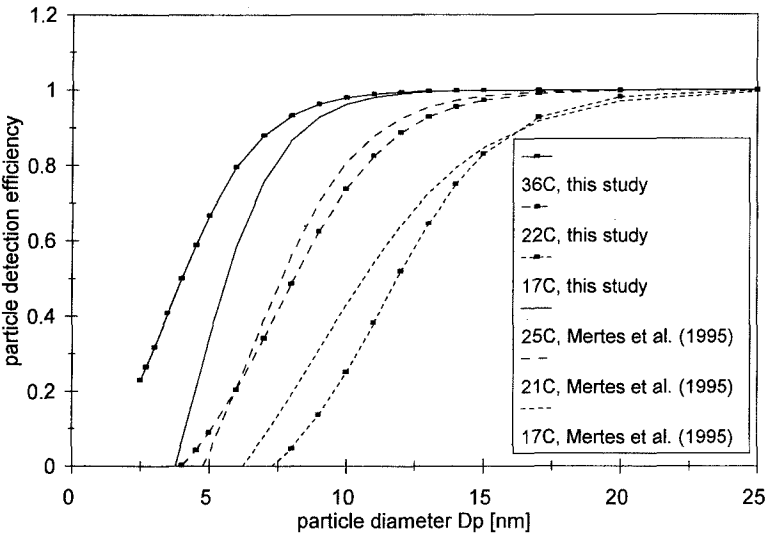

FIGURE 10. The average counting efficiencies of the TSI-3010 for different ΔTs obtained in this study compared to previous measurements. The solid, dashed, and dotted lines emphasized by solid squares represent the fitted counting efficiency curves for different ΔTs (17, 22, and 36°) in this study, and the solid, dashed, and dotted lines (17, 21, and 25°) represent the results by Mertes et al. (1995).

for 0.5 l/min, five for 1.0 l/min, and four for 1.5 l/min. Generally, the observed counting efficiency curves showed that with decreasing aerosol flow rate, the counting efficiency curve is shifted toward smaller particle sizes. For various reasons, however, not all counting efficiency curves measured were representative of the standard TSI-3760/7610 CPCs. Some data were therefore excluded. Specific reasons for excluding TSI-3760/7610 are as follows:

1. Two particle counters exhibited detection efficiencies larger than 100%: one (24) for 0.5 l/min, and another (16) for 1.0 l/min aerosol flow rate. With decreasing aerosol flow rate in the TSI-3760/7610 CPC, the residence time in the condenser becomes larger and, thus, particles may grow to larger butanol droplets. We observed that the pulses from the photodetector became too high and broad, leading to multiple counting and, subsequently, to an overestimation of the particle number concentration.
2. In two CPCs (18 and 19), the cavity of the saturator block was enlarged, leading to a longer residence time of the aerosol in the saturator, and probably to more butanol vapour being carried into the condenser. Subsequently, the supersaturation of butanol vapour became higher, leading to activation of smaller particles. The 50% detection efficiency diameter of these CPCs was shifted from 15 nm (nominal 50% detection efficiency diameter) to about 10 nm.
3. After calibration, we observed that one CPC (15) had irregularities in its electronics, probably leading to an inaccurate ΔT and, subsequently, to a shift in the 50% detection efficiency diameter.

The TSI-3760/7610 particle counters were investigated in terms of their counting efficiencies for different aerosol sample flow rates (0.5, 1.0, and 1.5 l/min; see also Table 5). The measured and fitted detection efficiency curves are shown in Figure 11a, b, and c for the aerosol flow rates 0.5, 1.0, and

TABLE 5. TSI-3760/7610 CPCs Calibrated during the Intercomparison Workshop

CPC Number	CPC Type	Institute	Serial Number	Aerosol Flow Rate (l/min)			Temperature Difference ΔT (°C)
15	TSI-3760	Univ. of Washington	389	—	1.0	—	17
16	TSI-3760	Univ. of Washington	495	—	1.0	1.5	17
18	TSI-3760	Univ. of Hawaii	580	—	—	1.5	17
19	TSI-3760	Univ. of Hawaii	243	—	—	1.5	17
21	TSI-7610	Lund Univ.	643	0.5	—	—	17
22	TSI-7610	Lund Univ.	644	0.5	1.0	1.5	17
24	TSI-7610	Lund Univ.	748	0.5	1.0	—	17
25	TSI-3760	Cape Grim	638	—	1.0	—	17

1.5 l/min, respectively. The coefficients of the exponential fits and 50% detection efficiency diameter for the different counters and operating conditions are listed in Table 6. In general, it was observed that the detection efficiency curve shifted to smaller particle sizes with decreasing aerosol flow rate.

These results are in contrast to Zhang and Liu (1991), who found a shift to larger particle sizes with decreasing aerosol flow rate. Our results show that the counting efficiency of the TSI-3760/7610 CPCs generally does not reach 100% for particles larger than 25 nm. The counting efficiencies we observed were between 90–98% for this size and are probably due to losses in the CPC. For the flow rate of 1.5 l/min (nominal 1.416 l/min), the nominal 50% detection efficiency diameter of 15 nm specified by the manufacturer was verified by our result. Furthermore, the slope of the detection efficiency curve becomes steeper with decreasing aerosol flow rate. This might be due to a more homogeneous temperature profile in the condenser and the larger butanol concentrations which may be achieved in the saturator.

CONCLUSION

An intercomparison study of the size-dependent counting efficiency of 26 condensation particle counters was performed during a calibration workshop in preparation for the Aerosol Characterization Experiment 1 (ACE1). Three different types of commercially available particle counters, the ultrafine condensation particle counter (TSI-3025 and the condensation particle counters TSI-3010 and TSI-3760 or TSI-7610), were investigated at default temperatures and flow settings as well as for other flow rates and temperature differences between the saturator and the condenser. The pulse-height-analysis ultrafine condensation particle counter and a TSI-3010 modified to achieve a higher temperature difference were also calibrated.

The average 50% detection efficiency diameter of the TSI-3025 UCPCs was determined to be 2.42 nm. This value is slightly smaller than the nominal one given by the manufacturer. The counting efficiency of some TSI-3025 UCPCs in the size range <5 nm seems to be influenced by disturbances of the laminar flow in the condenser tube due to dirt or butanol droplets. These flow disturbances led to a less steep counting efficiency curve. The shape of the counting efficiency curve of the properly functioning TSI-3025 UCPCs is very similar to the detection efficiency curve of the PHA-UCPC. In general, the aerosol flow of the TSI-3025 UCPC is not stable and should be frequently adjusted.

The 50% detection efficiency diameter of the PHA-UCPC was determined to be 2.49 nm. The modified TSI-3010 CPC with a ΔT of 36° between saturator and condenser exhibited a 50% detection efficiency diameter of 3.75 nm and reached a 90% counting

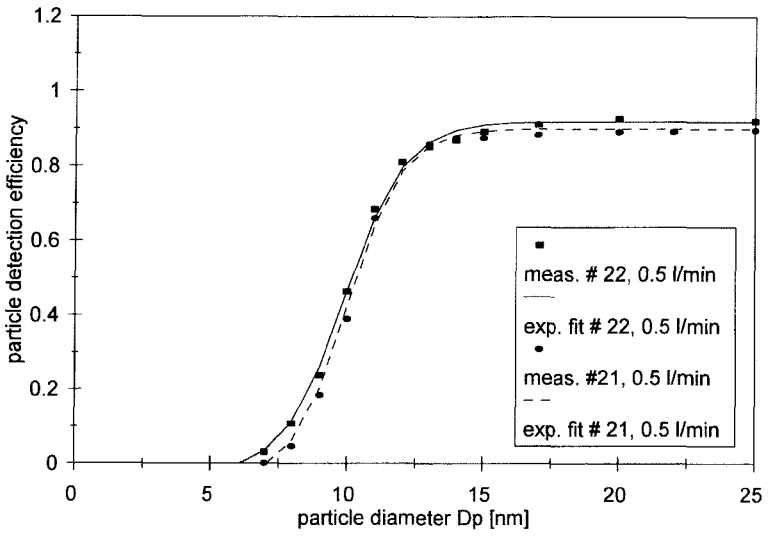

(a)

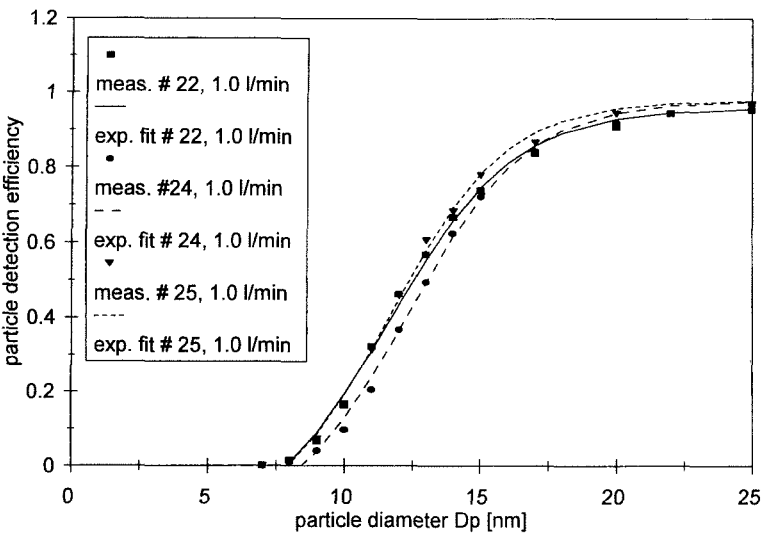

(b)

FIGURE 11. The measured and fitted counting efficiencies of TSI-37 60/7610 CPCs for different aerosol flow rates (0.5, 1.0, and 1.5 l/min). The solid squares, circles, and triangles represent the measured particle detection effidencies of various TSI-3760/7610 CPCs while the solid, dashed, and dotted lines represent the fitted counting efficiency curves.

efficiency at 10 nm. Furthermore, no homogeneous nucleation of butanol vapour was observed.

The average 50% detection efficiency diameters of the standard TSI-3010 CPC for $\Delta T = 17$ and 22°C were determined to be 11.9 and 8.15 nm, respectively. The shift of the counting efficiency curve to smaller particle sizes with increasing ΔT confirms previous measurements. The determined

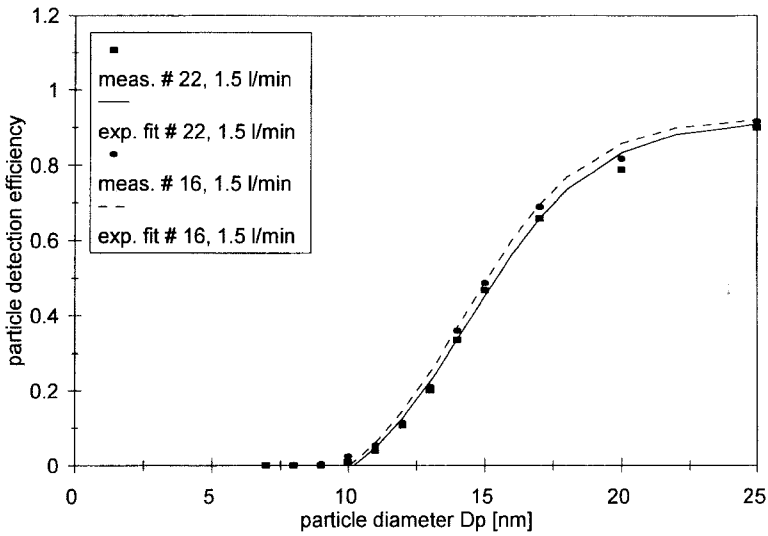

(c)

FIGURE 11. (*continued*)

50% detection efficiency diameters, however, are slightly different compared to the previous study.

The TSI-3760/7610 CPC was calibrated for three different aerosol flow rates: 0.5, 1.0, and 1.5 l/min. In contrast to previous investigations, we found that the 50% detection efficiency diameter shifted toward smaller particle sizes with decreasing aerosol flow rate. The 50% detection efficiency diameters were approximately 10.2, 12.3, and 15.2 nm for the aerosol flow rates 0.5, 1.0, and 1.5 l/min, respectively.

In general, the different particle counters are very sensitive to instrument conditions such as flow rate, temperature difference between saturator and condenser, or changes of the design. A frequent calibration for individual particle counters is required to characterise the exact counting efficiency spectrum for a given particle counter. This calibration is especially important when accurate, absolute concentration measurements are desired or when a comparison between two or more instruments is crucial.

TABLE 6. Coefficients of the Exponential Fit of Counting Efficiency Curves of the TSI-3760/7610 CPCs for Different Aerosol Flow Rates

CPC Number	CPC Type	Flow Rate (l/min)	b	a	D_1 (nm)	D_2 (nm)	$D_{p,50}$ (nm)
21	TSI-7610	0.5	0.90	0.95	10.0	1.0	10.32
22	TSI-7610	0.5	0.93	0.95	9.9	1.1	10.16
22	TSI-7610	1.0	0.95	1.12	11.6	2.2	12.53
24	TSI-7610	1.0	0.98	1.10	11.5	2.0	13.04
25	TSI-3760	1.0	0.98	1.10	11.8	2.0	12.37
16	TSI-3760	1.5	0.93	1.07	14.2	2.2	15.07
22	TSI-7610	1.5	0.92	1.07	14.4	2.3	15.40

The authors wish to thank the National Science Foundation for funding this intercomparison study as part of the Aerosol Characterization Experiment (ACE1), under grants ATM-9307603 and ATM-0311213. L.M.R. would also like to thank the Office of Naval Research (grant N00014-93-1-0872) and TSI, Inc. for supporting the development of the modified 3010 CPC.

References

Agarwal, J. K., and Sem, G. J. (1980). Continuous Flow, Single-Particle-Counting Condensation Nucleus Counter, *J. Aerosol Sci.* 11:343–357.

Birmili, W., Stratmann, F., Wiedensohler, A., Covert, D. S., Russel, L. M., and Berg, O. (1997). Determination of DMA Transfer Functions Using Identical Instruments in Series, *Aerosol Sci. Technol.* 27:215–223, accompanying article.

Fissan, H., Hummes, D., Stratmann, F., Büscher, P., Neumann, S., Pui, D. Y. H., and Chen, D. (1996). Experimental Comparison of Four Differential Mobility Analyzers for Nanometer Aerosol Measurements, *Aerosol Sci. Technol.* 24:1–13.

Hermann, M., and Wiedensohler, A. (1996). Modification and Calibration of a TSI 7610 Condensation Particle Counter for High Altitude Airborne Measurements, *J. Aerosol Sci.* 27S:303–304.

Kesten, J., Reineking, A., and Porstendörfer, J. (1991). Calibration of a TSI Model 3025 Ultrafine Condensation Particle Counter, *Aerosol Sci. Technol.* 15:107–111.

Mertes, S., Schröder, F., and Wiedensohler, A. (1995). The Particle Detection Efficiency Curve of the TSI-3010 CPC as a Function of the Temperature Difference Between Saturator and Condenser, *Aerosol Sci. Technol.* 23:257–261.

Russell, L. M., Caldow, R., Stolzenburg, M. R., Zhang, S. H., Flagan, R. C., and Seinfield, J. H. (1996). Radially-Classified Aerosol Discriminator for Aircraft-based Time-Resolved Ultrafine Size-Distribution Measurements, *J. Atmos. Ocean. Technol.* 13:598–609.

Saros, M. T., Weber, R. J., Marti, J. J., and McMurry, P. H. (1996). Ultrafine Aerosol Measurement Using a Condensation Nucleus Counter with Pulse Height Analysis, *Aerosol Sci. Technol.* 25:200–213.

Scheibel, H. G., and Porstendörfer, J. (1983). Generation of Monodisperse Ag- and NaCl-Aerosols with Particle Diameters Between 2 and 300 nm, *J. Aerosol Sci.* 14:113–126.

Stolzenburg, M. R., and McMurry, P. H. (1991). An Ultrafine Aerosol Condensation Nucleus Counter, *Aerosol Sci. Technol.* 14:48–65.

Weber, R. J. (1995). Studies of new particle formation in the remote troposphere, Ph.D. thesis, University of Minnesota.

Zhang, Z., and Lui, B. Y. H. (1991). Performance of TSI 3760 Condensation Nuclei Counter At Reduced Pressures and Flow Rates, *Aerosol Sci. Technol.* 15:228–238.

Received 28 May 1996; accepted 13 February 1997